IEEE Access
Multidisciplinary | Rapid Review | Open Access Journal

Received May 15, 2021, accepted May 23, 2021, date of publication June 4, 2021, date of current version June 29, 2021.

Digital Object Identifier 10.1109/ACCESS.2021.3086630

Recognition of Rock Micro-Fracture Signal Based on Deep Convolution Neural Network Inception Algorithm

GUILI PENG[1,3], XIANGUO TUO[2], TONG SHEN[3], AND JING LU[3], (Graduate Student Member, IEEE)

[1]School of Control and Mechanical, Tianjin Chengjian University, Tianjin 300384, China
[2]School of Automation and Information Engineering, Sichuan University of Science and Engineering, Zigong 643000, China
[3]School of Information Engineering, Southwest University of Science and Technology, Mianyang 621010, China

Corresponding authors: Xianguo Tuo (tuoxg@cdut.edu.cn), Guili Peng (planepeople678@sina.com), and Tong Shen (sht@swust.edu.cn)

This work was supported by the National Natural Science Foundation of China under Grant 41774188 and Grant 41704175.

ABSTRACT Rockburst is a common geological disaster in mines, tunnels, deep underground engineering, and during excavation, mining, and construction. Rockburst frequently occurs as the depth of burial increases, and its early warning technology is in urgent need of further development. At present, the most effective monitoring and analysis method of rockburst is microseismic technology, which detects a large number of rock micro-fracture signals through geophones. The identification of microseismic monitoring data is an essential part of microseismic data processing. It is necessary to identify effective microseismic signals from considerable monitoring data for subsequent early warning. Aiming at the identification of rock micro-fracture signals, this thesis proposes a microseismic data identification method based on the Deep Convolution Neural Network Inception (DCNN-Inception) algorithm. The algorithm uses an existing Convolutional Neural Network (CNN) model, adding Inception structure in the middle of the model to form a DCNN-Inception model. A data set was established depending on the actual measured data of Baihetan Hydropower Station, and CNN and DCNN-Inception were employed to identify effective microseismic signals. The results demonstrate that the DCNN-Inception algorithm is better than CNN in recognition accuracy and can effectively identify effective microseismic signals. It provides an essential foundation for the identification of microseismic abnormal signals of rock microfracture and the early warning of rock rupture precursors and is of practical significance for the study of rockburst warning technology.

INDEX TERMS Rock micro-fracture signals, deep convolution neural network, inception structure, microsiesmic signal recognition, accuracy and loss rate.

I. INTRODUCTION

With the development of China's economy and the strategy of large-scale development of the western region, the society's demand for various resources continues to rise, and the scale of resource extraction continues to expand. Southwestern China has huge reserves of oil and gas resources, mineral resources, and hydropower resources, which need to be extensively developed and utilized. Its development intensity and construction scale have developed to the deep underground [1]–[5]. Consequently, engineering geological disasters caused by deep problems are increasing. The rockburst problem induced by high ground stress is the most prominent. Rockburst is the sudden and violent release of the elastic strain energy accumulated in the hard and brittle rock mass under the action of construction excavation and unloading under high ground stress conditions, causing the rock to burst and eject. This leads to problems such as falling rocks, landslides, tunnel collapse, casualties, economic losses, and cracks in the construction of the foundation. How to effectively predict and prevent rock bursts has become the common focus of underground engineering construction and rock mechanics research. Microseismic monitoring is a new type of monitoring technology developed internationally in the 1990s for the rockburst phenomenon of deep-buried tunnels [6]–[8]. It can be used for geological

The associate editor coordinating the review of this manuscript and approving it for publication was Jin-Liang Wang.

disaster monitoring, mine pressure monitoring, and stability monitoring of deep-buried tunnels. The principle is to first receive microseismic signals generated by rock mass rupture through arranging geophone arrays in certain areas; second, the time-frequency analysis method is used to obtain information such as the time and source intensity of the microseismic event; finally, the location algorithm is used to accurately locate the microseismic event, determine the development location of the rock mass fracture surface, and evaluate the frequency of microseismic events in a certain area and the source intensity to realize the function of tunnel excavation rockburst disaster prediction. However, the current microseismic signal acquisition process is usually accompanied by project construction, and there is a certain chance that interference signals such as artificial blasting, mechanical construction vibration, and environmental noise will be collected. The energy of these signals is usually much greater than that of microseismic signals, resulting in submerging useful signals. The signal collected by the geophone is a mixture of microseismic signals and interference noise signals [9]–[11]. How to quickly and accurately separate the microseismic signal from it and effectively and accurately identify plays a significant role in the location of rock fracture micro-seismic events and is the premise of tunnel excavation rockburst prediction. The research on the recognition algorithm of microseismic signals is of great significance.

The micro-seismic monitoring technology can delineate disaster risk areas in time through real-time monitoring of rock mass rupture, realizing disaster prediction and prevention to a large extent. This plays a crucial role in reducing casualties and in some apartments such as geological disaster monitoring, mining, and mine safety. In the recognition of microseismic events, researchers worldwide have conducted many years of research and have achieved many significant research results. Longjun *et al.* [12] used time-frequency analysis to discover that the main frequency of microseisms is 18-70Hz, the main frequency of artificial blasting is 60-100Hz, and the main frequency of electrical noise is 50Hz. Allmann *et al.* [13] used the Fourier transform method to investigate periodic stationary signals and obtained the amplitude-frequency characteristics of the mine microseismic signal, providing a foundation for preliminary identification of rock rupture and blasting vibration signals. Quan-Jie and Fu-Xing [14] studied microseismic signals and revealed that the energy of blasting signals and the energy of rock rupture signals were mostly concentrated at 375-500Hz and 0-125Hz, respectively. Guoyan *et al.* [15] explored the dimensions of microseismic signals and discovered that the box dimensions of blasting signals are mainly distributed in 1.5-1.6; the box dimension of the rock micro-fracture signal is mainly distributed below 1.4; the box dimensions of electromagnetic interference microseismic signals are concentrated in 1.7-1.8. Wenwu *et al.* [16] used Fourier transform to analyze the blasting and microseismic signals and obtained the power spectrum and amplitude-frequency characteristics, revealing that the microseismic signal reached the maximum amplitude in the range of 20-30Hz, and the blasting signal reached the maximum amplitude at 10Hz. Regarding the recognition of microseismic signals, with the development of pattern recognition and artificial intelligence, computer software, SVM, linear discriminant, and Bayesian methods have been used to recognize microseismic signals. Dargahi-Noubary [17] established a non-stationary stochastic model to build an earthquake identification model and construct a secondary identification. Marambio *et al.* [18] applied logistic regression and neural network to the recognition of microseismic and blasting events and constructed a recognition model with 13 waveform parameters as characteristic values. Jeffrey *et al.* [19] constructed a microseismic event classification and recognition model based on principal component analysis by extracting the frequency domain characteristics, duration characteristics, and statistical characteristics of microseismic events, and its classification accuracy rate reached 90%-95%.

In recent years, with the development of artificial neural networks and image recognition, more and more pattern recognition methods have been used by researchers in microseismic data recognition research. Quanjie *et al.* [20] established an algorithm for range and scale-free fractal box size by studying the fractal characteristics of microseismic signals to identify mechanical vibration waveforms, blasting waveforms, and rockburst waveforms of SVM networks. Professor Yinju applied the genetic neural network algorithm to natural earthquakes and artificial blasting events early on [21]. CNN algorithm is currently one of the most commonly used algorithms in the field of image recognition research. In 1998, LeCun proposed CNN. In 2012, Hinton's research team used the CNN model to participate and won the championship of the I-mageNet image classification competition. To solve the problem of distinguishing gastric cancer and gastritis from magnifying endoscopy (MENBI), and narrowband imaging, Horiuchi *et al.* [22] presented a ME-NBI image classification scheme based on CNN image recognition. The experimental results indicated that the accuracy of the scheme can reach 85.3%. Besides, Salgado *et al.* [23] put forward a high-precision automatic classification system for eight groups of peripheral blood cells using the CNN-Inception method, and the experiments revealed that its accuracy rate was 86% when using Vgg-16 to extract features. Dokht *et al.* [24] provided an CNN algorithm based on double optimization to improve the recognition accuracy and convergence speed of the CNN algorithm. Liao Enhong *et al.* proposed a new food image recognition model, China Food-CNN, and adopted CNN recognition to accurately classify food. The experimental results demonstrated that the model's recognition accuracy of food images was 69.2% [25]. Hong *et al.* [26] presented a small sample bark image recognition scheme based on CNN to solve the problems of few image training samples and low recognition rate in the process of bark image classification. The experimental results indicated that the accuracy of the scheme on the MNIST data set, ImageNet data set, and the CIFAR-10

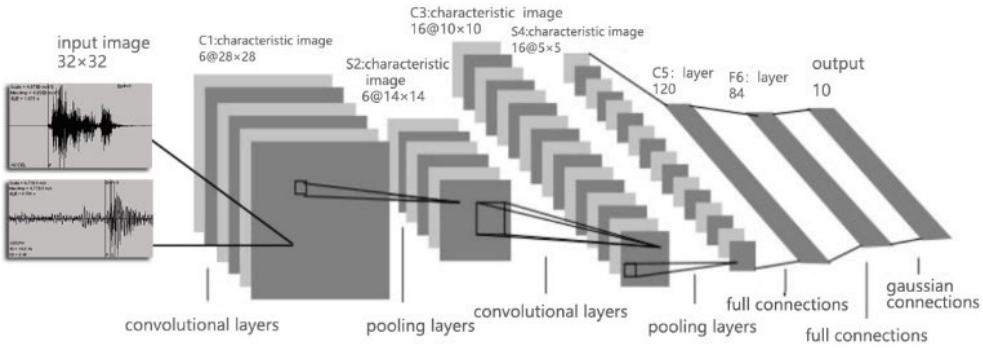

FIGURE 1. Structure model of CNN for microseismic signals. Convolutional neural network includes input layer of microseismic image, convolution layer of feature extraction, pooling layer of feature compression, full connection layer of information connection and final classifier layer.

data set was 92%, 90%, and 93%, respectively. Furthermore, Jiazheng *et al.* [27] offered a scheme of breast histopathological image classification based on CNN and wavelet decomposition images.

This paper proposes a method of using CNN to recognize images to process microseismic data. CNN has long been one of the core algorithms in the field of image recognition and can effectively handle some large-scale data classification problems. During the rock microseismic monitoring process, a quantitative data signal is generated. The signal is three-component microseismic data and interference noise data, with certain characteristic parameters. Then, these characteristic parameter data are visualized to form a picture data set. Next, CNN is employed to extract feature values in the picture and perform classification learning. Particularly, feature extraction can manually input images of different categories into CNN. Finally, the test set is classified. On this basis, deep learning is added, the network structure is migrated, and the DCNN-Inception network is formed. The above steps are repeated to complete the identification of microseismic signals. At present, the test results indicate that the accuracy of DCNN-Inception can reach more than 90%, which is better than that of the ordinary CNN model.

II. METHOD AND DATASET SOURCE

A. CONVOLUTIONAL NEURAL NETWORK FUNDAMENTALS IN MICROSEISMIC SINGLE

The full name of the CNN algorithm is convolutional neural network, which is a feedforward neural network. It is generally composed of a data input layer, a convolutional calculation layer, a pooling layer, and a fully connected layer. It is a neural network using convolutional operations to replace traditional computing methods [28]–[32]. The network structure model of CNN is illustrated in Figure 1.

The data input layer mainly inputs the microseismic signals image. The convolutional layer is for microseismic image's feature extraction. The feature value can be obtained using the convolution kernel to extract the features of the image. The convolution formula is expressed as formula 1:

$$z(x, y) = f(x, y) * g(x, y) = m\sum\nolimits_{n} f(x-m, y-n) * g(m, n) \tag{1}$$

The pooling layer is for microseismic image's feature compression to extract main features. The fully connected layer connects all the features together using softmax function [33]–[35]. The commonly used classification method is expressed as formula 2:

$$y1 = f(w(x-1)+b)) \tag{2}$$

The mathematical expression of Softmax is provided in formula 3:

$$a_j^L = \frac{e_j^L}{\sum_k e^{Z_k^L}} \tag{3}$$

B. ROCK MICROSEISMIC DETECTION AND DATA SOURCE

In the rock micro-seismic monitoring system for deep-buried tunnels, the first step is to collect micro-seismic events collected at the construction site. The signals collected by microseismic events mainly include microseismic signals and interference noise signals. The source of the microseismic monitoring signal is the microseismic monitoring activity during the construction of the 1# tailrace tunnel of the Upper Baihetan Hydropower Station on the Jinsha River at the junction of Sichuan and Yunnan, China. The main monitoring location is exhibited in Figure 2.

The monitoring geophone is installed near the excavation face. After the microseismic sensor is installed, the host monitoring device is placed in a suitable location. In the monitoring of the tailwater construction branch tunnel, the instrument is placed at the point of avoid the explosion. In the monitoring of the tailwater connecting tunnel, the instrument is placed in the tailwater construction branch hole that has been excavated. Besides, the connection status of the system was tested after completing the instrument installation. The monitoring instrument host installation diagram and microseismic sensor installation diagram are illustrated in Figure 3.

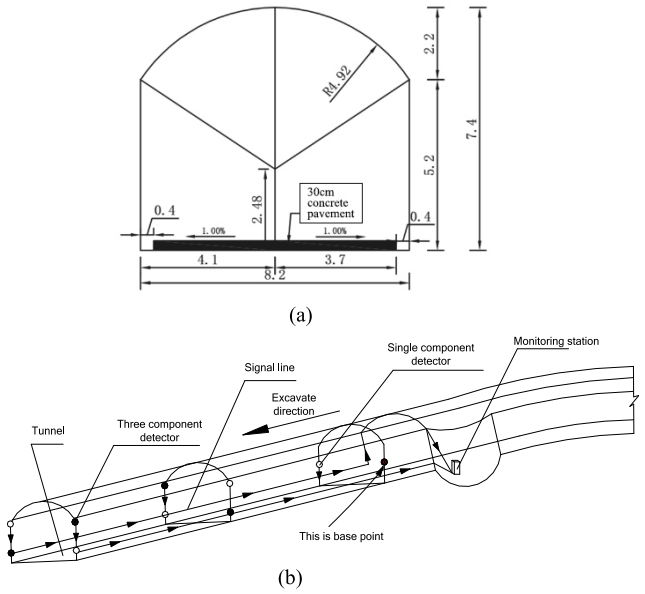

FIGURE 2. (a) Monitoring cavern plane graph. The tailrace tunnel is arched and its dimensions are indicated in the graph. (b) Monitoring cavern location graph. The blank circle represents the single component sensor position, the black real circle represents the three component sensor position, and the cube represents the monitoring station position.

FIGURE 3. (a) Monitoring system installation. It is real monitoring equipment. (b) Monitoring cavern condition. It is a real photo of the monitoring site.

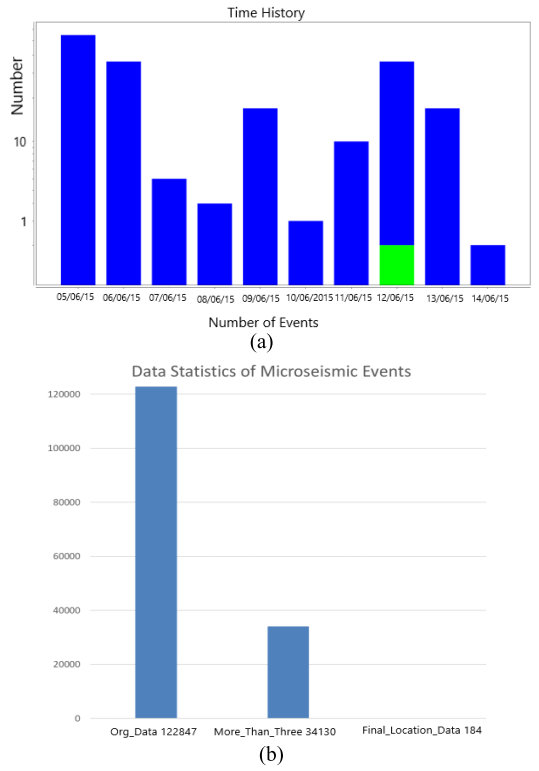

FIGURE 4. (a) Time history of microsiesmic event number. It is a 24-hour statistical chart of system monitoring. Blue represents that the magnitude energy of microseismic is less than 1.0, and green represents that the energy is greater than 1.0 (b) Statistical chart of microsiesmic event detection. It represents the total statistical quantity of microseismic data, including original data, effective events and final positioning.

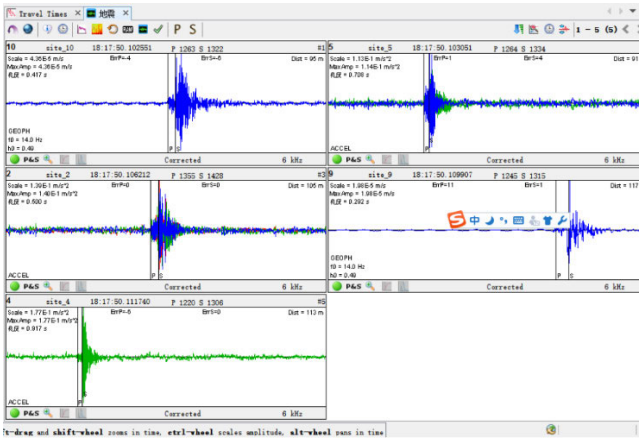

FIGURE 5. Waveform of microseismic signals on the monitoring software. It describes the signals of the same microseismic event detected by multiple sensors. Blue, green and red represent the waveforms obtained by the three component detector respectively, and monochrome is the single component detection waveform.

The microseismic monitoring period is from June 1, 2017, to November 5, 2017, about 5 months. There are 506,485 microseismic events monitored, and 32,562 effective microseismic events can be identified. To avoid the repetitiveness of the recorded data, the microseismic signals are collected in time series, with a certain degree of randomness, temporality, and some Gaussian noise. The main collection for a period of time is the statistics of microseismic events, as presented in Figure 4.

It can be observed from the monitored microseismic events that the collected microseismic signals are all mixed three-component signals, including multiple signals and interference noise signals. In the monitoring software, there are monitoring information of single-component detectors and three-component detectors. The signals are showed more geophones in a microseismic event are illustrated in Fig. 5.

The mixed signal of active source signal and microseismic signal produced by blasting event can be found in Figure 7. It is known that the seismic source is on the heading face. The

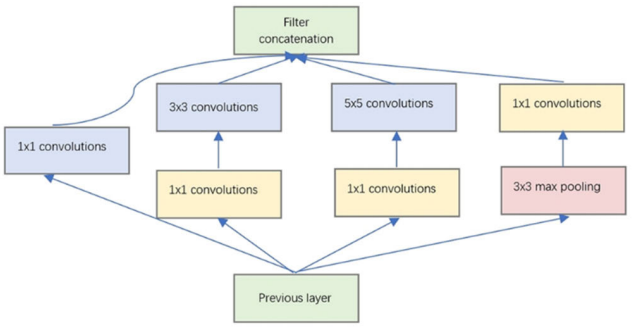

FIGURE 6. DCNN-Inception network structure diagram. The structure consists of four 1*1 convolutions, two 3*3 convolutions and one 5*5 convolution, which are connected according to the graph to form the structure.

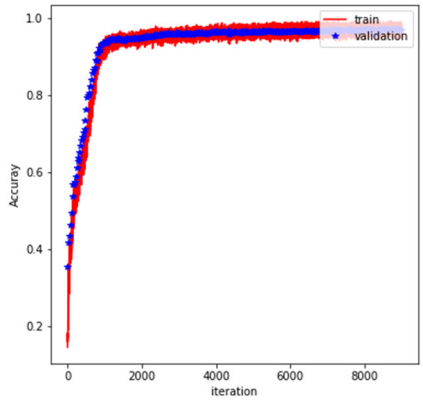

FIGURE 7. Accuracy graph of CNN network recognition based on training set and validation set. Red line represents the training set data, and blue line represents the verification set data. The data reached 90% after 700 iterations, and finally reached 91.2%.

microseismic events, the waveform, starting time, amplitude and travel time of the collected microseismic signals can be observed in the monitor.

The data set contains microseismic data, active source data and noise data. In other classified databases, 60% of the extracted data is used as training set for training network, 30% of the extracted data set is used for verification, and the remaining 10% is used for testing.

C. THE PRINCIPLE OF DEEP CONVOLUTIONAL NEURAL NETWORK INCEPTION

DCNN-inception, also known as inception learning, is also a CNN model. This architecture increases the depth and width of the network with a small amount of calculation. Simply increasing the model depth will cause the model to be too large, too many parameters, and easily over-fitting. The solution can be to replace full connections using sparse connections, or even replace the convolutional layer with a sparser convolution. For the Inception model structure, the sparse parameter reduction effect can be achieved, and the performance of the dense matrix optimization in the hardware can also be used. The main idea is to find the optimal

TABLE 1. DCNN-Inception structure for microseismic event recognition.

layer	type	Kernel Size	STRIDE	Output
1	Input	—	—	3 maps of 128*128 neurons
2	CovRelu1	5*20	—	16 maps of 118*122 neurons
3	CovRelu2	5*20	—	16 maps of 78*96 neurons
4	Maxpool1	2*2	(2,2)	16 maps of 58*76 neurons
5	CovRelu3	5*20	—	16 maps of 38*46 neurons
6	CovRelu4	5*20	—	16 maps of 28*36 neurons
7	Maxpool2	2*2	(2,2)	16 maps of 17*23 neurons
8	Mixed1-10	—	—	—
9	Maxpool3	2*2	(2,2)	16 maps of 6*10 neurons
10	FC1-2	—	—	188 neurons
11	Softmax	—	—	3 neurons

local sparse structure in the convolutional visual network that can be approximated. Using a large convolution kernel will spread more regions in space. Consequently, the corresponding clusters will decrease, and the number of clusters will decrease as the convolution kernel increases. To avoid this problem, the output filter bank with multiple convolutional layers added to the Inception structure will be concatenated into a filter bank [36]–[38]. The specific structure is exhibited in Fig. 6.

The 4 branches of DCNN-Inception were merged through an aggregation operation at the end, and a very efficient sparse structure conforming to the Hebbian principle was constructed. It contains three different sizes of convolution and a maximum pooling, increasing the adaptability of the network to different scales, improving accuracy, and preventing overfitting. It has multiple stacked structures. Therefore, in the last few layers of the entire model, their spatial concentration will decrease when higher abstract features are captured by higher layers. The filter structure using multi-core convolution can help extract features in more detail and improve accuracy [39]–[41]. The DCNN-Inception microseismic signal recognition network designed in this paper mainly includes an input layer, 4 convolutional layers, 3 maximum pooling layers, 10 mixed Inception layers, 2 fully connected layers, and 1 softmax output layer. Each of the 10 mixed layers includes an AvgPool layer, two Conv layers, a max pool layer, and a Fully Connect layer.

The network structure is presented in Table 1. Specifically, the number of microseismic categories is 2, the number of channels is 3, the number of training data is 5000, the number of training steps is 100, the learning rate is 0.01, and the computer used is Intel(R) Core(TM) i7-6700HQ 2.60GHz (CPU), 16G memory. It took 1.5 hours to complete the microseismic signal identification work. The network structure of the DCNN-Inception algorithm is provided in Table 1:

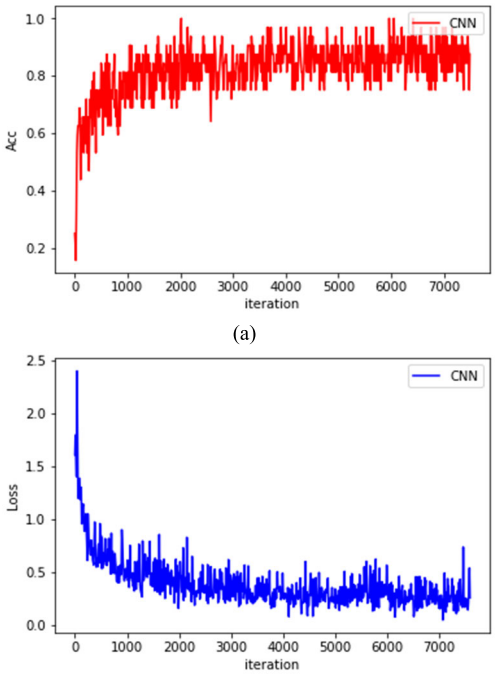

FIGURE 8. (a) Accuracy rate of CNN network recognition. (b) Loss ate of CNN network recognition. The recognition accuracy is 85.3% and the loss rate is 30.4%.

III. RESULT

The established CNN neural network is used for training and recognition. First, the microseismic data collected at Baihetan is converted from ASC format to XLS format. Then, the data in XLS is read into a NumPy array format. The different signal data is randomly distributed in 35524 microseismic events; 60% of the data is taken as the training data, 30% of the data is taken as the validation set data, and 10% of the data is taken as the test set after the model training is completed. Then, data training is performed on the model of the set network parameters. After 1 hour of training and more than 20 iterations of training, the recognition accuracy of the training set reached more than 90%, and the operation was stopped. Afterward, the verification is performed on the data added to the verification set. Fig.7 presents the accuracy of CNN network recognition on the training set and validation set data.

Finally, the trained and verified CNN network is tested, and the test set data is input into the established recognition network. The specific recognition accuracy and loss rate are exhibited in Fig. 8.

The curve is displayed on the test set. After 5000 iterations of the data, the step size is 100. Then, the CNN network model is basically balanced, and it makes no sense to perform calculations backward. The accuracy rate and the loss rate remained at 0.853 and 0.304, respectively. Therefore, the recognition effect of CNN network training achieves the goal, and the ideal recognition effect is obtained.

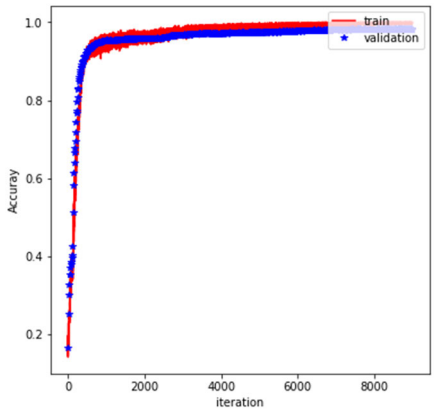

FIGURE 9. Accuracy graph of DCNN-Inception network recognition based on training set and validation set. Red line represents training set data and blue line represents verification set data. The data reaches 90% after 200 iterations, and finally reaches 95.8%.

Based on the established four-layer convolutional CNN network, the Inception structure is added to identify the microseismic data of Baihetan to verify whether the network is better than the CNN network. The data set is imported in the same NumPy array format. Then, the data is divided into a training set, validation set, and test set in turn. The data is trained through the set network parameters. When the network is iterated to 100 times, the recognition accuracy of the training set reaches 0.95. Stop the calculation, and then the data added to the verification set is verified. The accuracy of DCNN-Inception network recognition on training set and validation set data is illustrated in Fig. 9.

In the research of DCNN-Inception recognition accuracy of training set and verification set, it is found that the accuracy of the network has exceeded 80% after about 200 iterations and 95% after about 700 iterations.

Finally, the trained and verified CNN-Inception network is tested, and the test set data is input into the established recognition network. The specific recognition accuracy and loss rate are presented in Fig. 10.

The curve is displayed on the test set. The accuracy rate rose slowly in the iterative process. After 5000 iterations of the model, there is no stable situation in the CNN network. Therefore, we decided to adjust the step size to 300. The model began to converge after 12,000 iterations. The final model accuracy reached 0.924 on the verification set, and the loss was reduced to 0.174. The accuracy of the model has been improved a lot after the network parameters were modified. This fully verifies that the network with the DCNN-Inception structure can extract more detailed features, and the classification ability of the model is significantly improved.

IV. DISCUSSION

We established a data set of the mixed data of microseismic and noise in the microseismic event monitored by Baihetan Hydropower Station and used the CNN network and

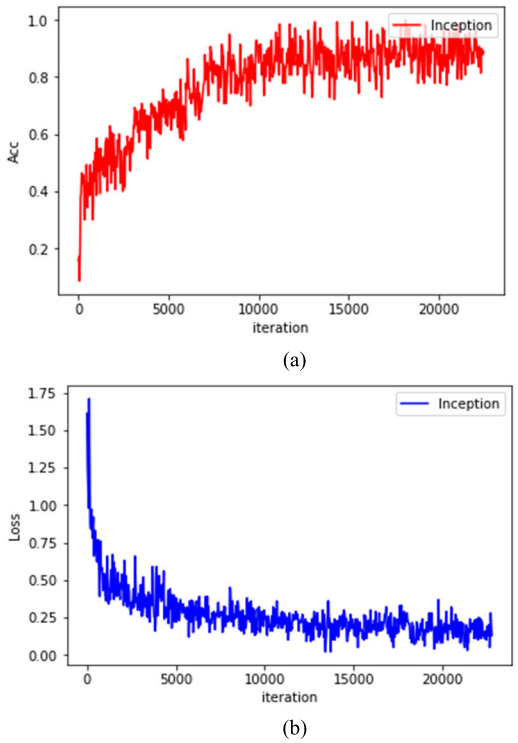

FIGURE 10. (a) Accuracy rate of DCNN-Inception network recognition. (b) Loss rate of DCNN-Inception network recognition. The recognition accuracy is 92.4% and the loss rate is 17.4%.

TABLE 2. Recognition of microseismic signals by CNN and DCNN inception networks.

	Training set	validation set	Testing set
Accuracy rate of CNN	0.912	0.912	0.853
Accuracy rate of DCNN-Inception	0.958	0.958	0.924
Loss rate of CNN	0.334	0.334	0.304
Loss rate of DCNN-Inception	0.152	0.152	0.174

TABLE 3. Application of two networks using different methods of identification results (Event: data legth 3000).

Data group	CNN algorithm	DCNN-inception algorithm
Batch size	32	32
Learning rate	0.01	0.005
Iteration period	20	300
Loss rate	0.334	0.152
Accuracy rate	0.912	0.958
Learning time	1h	4.5h

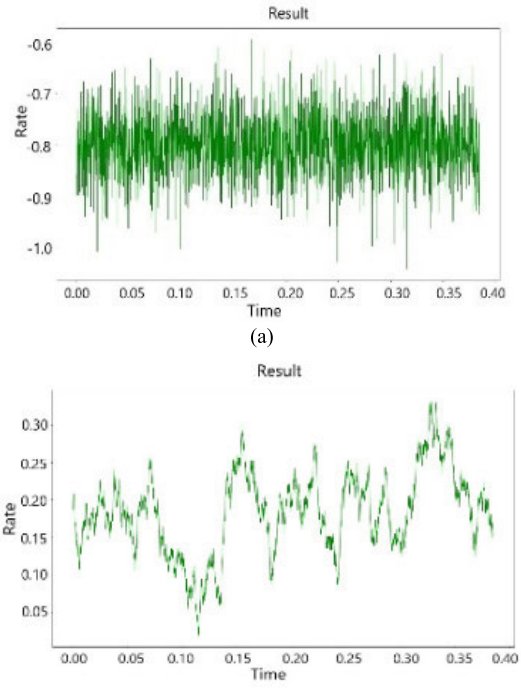

FIGURE 11. (a) The white noise data image. (b) The random noise data image. Gaussian white noise is regular and has the same number of extreme points. Random noise is irregular, random and uncertain.

DCNN-Inception network for identification. The network parameters are trained and constructed through the training set and the validation set. The accuracy rate obtained is provided in Table 2.

The effects of different learning aspects of two different DCNN-Inception algorithms on the recognition effect are compared, and the main recognition results are presented in Table 3:

As demonstrated by the above two tables, the CNN network has a simple structure and its training speed is better than that of the DCNN-Inception network; it only took 1 hour to complete the training, and the accuracy rate on the validation set reached a height of 0.90; besides, the model started to reach the optimal solution after 5000 iterations. The DCNN-Inception network structure is complex; after 300 steps, the training time reached 4.5 hours; after 16000 iterations, the result was obvious convergence; an accuracy of 0.924 was achieved on the verification set, and the loss was reduced to 0.174. Compared with the CNN network structure, the accuracy of the DCNN-Inception model is increased by 2.4%. Although the training time of DCNN-Inception is long, the feature fitting ability of microseismic data is stronger than that of the CNN network, the feature extraction ability is strong, and the accuracy rate is significantly improved.

In order to improve the recognition accuracy of DCNN network, and further improve the data set. The research used Python language code to generate a large number of random and Gaussian white noise to enhance the data set. This method makes the data set more robust and completes the data expansion. The generated image is shown in Figure 11.

The DCNN algorithm is established in this paper. The main algorithm flow chart is shown in Figure 12.

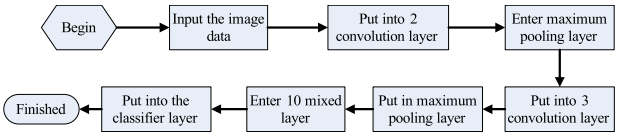

FIGURE 12. DCNN algorithm flowchart. The algorithm flow mainly includes the input layer of image data, 2-layer convolution layer of feature extraction, maximum pooling layer of feature compression, 3-layer convolution and 1-layer maximum pooling layer of further feature extraction, and then 10 layer hybrid migration layer, which is used to optimize the network, suppress over fitting, and finally enter the classifier layer for classification.

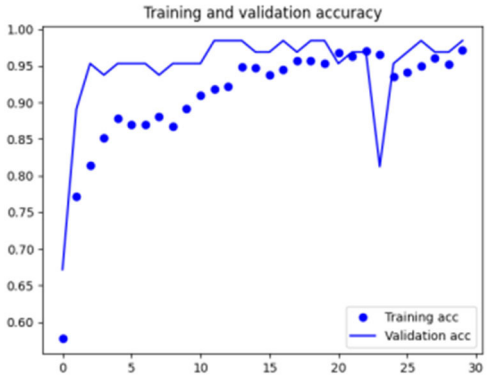

(a)

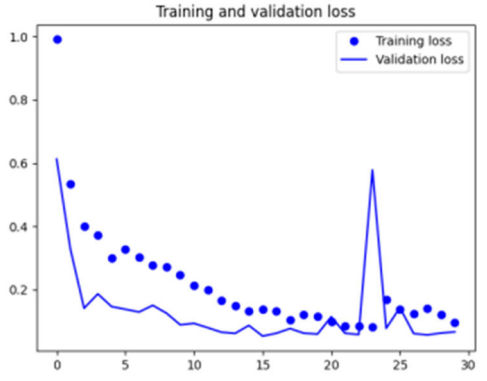

(b)

FIGURE 13. (a) Accuracy rate of CNN network using training set and verification set compare. (b) Loss rate of CNN network using training set and verification set compare. The dot represents the training set data and the line represents the verification set data. The fluctuation of the verification set is larger than the training set, the recognition accuracy is 95%, and the loss rate is 9.8%.

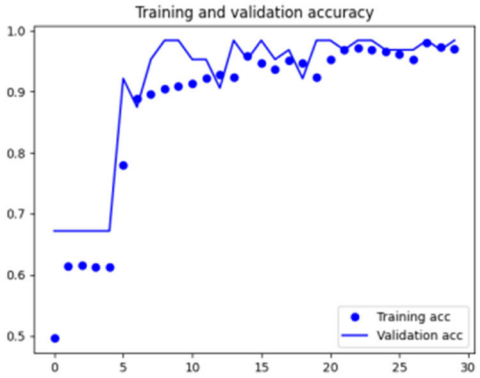

(a)

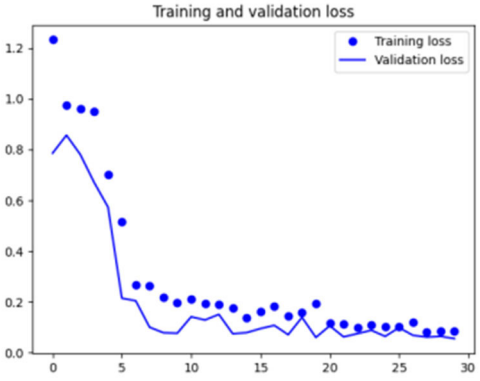

(b)

FIGURE 14. (a) Accuracy rate of DCNN-Inception network using training set and verification set compare. (b) Loss rate of DCNN-Inception network using training set and verification set compare. The dot represents the training set data and the line represents the verification set data. The fluctuation of the verification set is consistent with that of the training set, the recognition accuracy is 98.2%, and the loss rate is 8.6%.

TABLE 4. The results of DCNN-INCEPTION algorithm classification by confusion matrix method.

True\Test	Active blasting source	Microseismic signal	Noise
Active blasting source	24	6	2
Microseismic signal	3	32	1
Noise	1	0	22

In order to further explain the algorithm, we randomly select data from the collected data set to verify the two algorithms, and calculate the accuracy and loss rate using the training set and the test set. The main figures are shown in figures 13 and 14.

In order to further explain the recognition effect of DCNN-Inception algorithm, the researchers used confusion matrix method to analyze the classification results, mainly randomly selected data from the collected data for testing. The main analysis results are shown in Table 4.

V. CONCLUSION

In this paper, the one-year microseismic monitoring data of Baihetan Hydropower Station is used as the main research object, the collected microseismic signals and noise signals in the microseismic events are taken as the data set, and CNN network and DCNN-Inception network are employed to identify the signals. It can be concluded that both convolutional neural network algorithms can identify the microseismic event. Specifically, the DCNN-Inception model algorithm is better than the CNN network in recognition accuracy.

However, its training time is longer, and a large amount of data is needed to perfect the network. Its network model has strong feature extraction capabilities for microseismic data and can effectively identify microseismic signals. This provides an essential foundation for the identification of microseismic anomaly signals and early warning of rock micro-fracture, and it is of practical significance for the investigation of rockburst early warning technology.

DATE AND RESOURCES

In this work, the microseismic data is from monitor detection in BaiHetan Hydropower Station 1# tunnel tube in this study. The time period of microseismic monitoring data of BaiHetan Hydropower Station is from May to October in 2018. We use CNN-inception framework for Python, to train deep convolutional networks at the github website. These dates do not involve a conflict of interest.

CONFLICT OF INTEREST

We declare that we have no financial and personal relationships with other people or organizations that can inappropriately influence in this paper. There is no professional or other personal interest of any nature or kind in any product. We confirm that there is no conflict of interest regarding the publication in this paper, and declare that there is no conflict of interest regarding the publication of this paper.

REFERENCES

[1] M. F. Abdelwahed, "SGRAPH (SeismoGRAPHer): Seismic waveform analysis and integrated tools in seismology," *Comput. Geosci.*, vol. 40, pp. 153–165, Mar. 2012.
[2] P. B. Quang, P. Gaillard, Y. Cano, and M. Ulzibat, "Detection and classification of seismic events with progressive multi-channel correlation and hidden Markov models," *Comput. Geosci.*, vol. 83, pp. 110–119, Oct. 2015.
[3] G. M. Atkinson, D. W. Eaton, H. Ghofrani, D. Walker, B. Cheadle, R. Schultz, R. Shcherbakov, K. Tiampo, J. Gu, R. M. Harrington, and Y. Liu, "Hydraulic fracturing and seismicity in the western Canadasedimentary basin," *Seismol. Res. Lett.*, vol. 87, no. 3, pp. 631–647, 2016.
[4] S. A. Barrett and G. C. Beroza, "An empirical approach to subspace detection," *Seismological Res. Lett.*, vol. 85, no. 3, pp. 594–600, May 2014.
[5] Y. Bengio, A. Courville, and P. Vincent, "Representation learning: A review and new perspectives," *IEEE Trans. Pattern Anal. Mach. Intell.*, vol. 35, no. 8, pp. 1798–1828, Aug. 2013.
[6] C. D. Saragiotis, L. J. Hadjileontiadis, and S. M. Panas, "PAI-S/K: A robust automatic seismic p phase arrival identification scheme," *IEEE Trans. Geosci. Remote Sens.*, vol. 40, no. 6, pp. 1395–1404, Jun. 2002.
[7] N. Srivastava, G. Hinton, A. Krizhevsky, I. Sutskever, and R. Salakhutdinov, "Dropout: A simple way to prevent neural networks from overfitting," *J. Mach. Learn. Res.*, vol. 15, no. 1, pp. 1929–1958, 2014.
[8] J. F. Tan, H. C. Bland, and R. R. Stewart, "Classification of microseismic events from bitumen production at cold lake," *Alberta CREWES Res. Rep.*, vol. 19, pp. 1–24, Dec. 2007.
[9] Y. Xue, C. Bai, D. Qiu, F. Kong, and Z. Li, "Predicting rockburst with database using particle swarm optimization and extreme learning machine," *Tunnelling Underground Space Technol.*, vol. 98, pp. 103287.1–103287.12, Apr. 2020.
[10] S. Gaci, "The use of wavelet-based denoising techniques to enhance the first-arrival picking on seismic traces," *IEEE Trans. Geosci. Remote Sens.*, vol. 52, no. 8, pp. 4558–4563, Aug. 2014.
[11] R. Schultz, V. Stern, and Y. J. Gu, "An investigation of seismicity clustered near the Cordel field, west central alberta, and its relation to a nearby disposal well," *J. Geophys. Res. Solid Earth*, vol. 119, no. 4, pp. 3410–3423, Apr. 2014.
[12] D. Longjun, S. Daoyuan, L. Xibin, M. Ju, C. Guanhui, and Z. Chuxuan, "Statistical identification method and engineering application of microseismic and blasting events," *J. Rock Mech. Eng.*, no. 7, pp. 1423–1433, 2016.
[13] B. P. Allmann, P. M. Shearer, and E. Hauksson, "Spectral discrimination between quarry blasts and earthquakes in southern california," *Bull. Seismological Soc. Amer.*, vol. 98, no. 4, pp. 2073–2079, Aug. 2008.
[14] Z. Quan-Jie and J. Fu-Xing, "Classification of mine microseismic events based on wavelet-fractal method and pattern recognition," *Chin. J. Geotechn. Eng.*, vol. 2012, no. 34, pp. 2036–2042, 2012.
[15] Z. Guoyan, D. Qinglin, and M. Ju, "Analysis and identification of coal mine microseismic signal based on fswt time-frequency analysis," *Chin. J. Geotechn. Eng.*, vol. 2015, no. 2, pp. 306–312, 2015.
[16] J. Wenwu, Y. Zuolin, X. Jianmin, and L. Jiafu, "Application of FFT spectrum analysis to identify microseismic signals," *Sci. Technol. Rev.*, vol. 33, no. 2, pp. 86–90, 2015.
[17] G. R. Dargahi-Noubary, "Identification of seismic events based on stochastic properties of the short-period records," *Soil Dyn. Earthq. Eng.*, vol. 17, no. 2, pp. 101–115, Feb. 1998.
[18] E. Marambio, J. A. Vallejos, L. Burgos, C. Gonzalez, L. Castro, J. P. Saure, and J. Urzua, "Numerical modelling of dynamic testing for rock reinforcement used in underground excavations," in *Proc. 4th Int. Symp. Block Sublevel Caving*, Y. Potvin and J. Jakubec, Eds. Perth, WA, Australia: Australian Centre for Geomechanics, 2018, pp. 767–780.
[19] F. T. Jeffrey, R. S. Robert, and W. Joe, "Classification of microseismic events via principal component analysis of trace statistics," *CSEG Recorder*, vol. 2010, no. 1, pp. 34–38, 2010.
[20] Z. Quanjie, F. Jiang, Z. Yu, and Y. Yin, "Study on energy distribution characteristics of microseismic signals in blasting vibration and rock fracture," *J. Rock Mech. Eng.*, vol. 314, pp. 723–730, Apr. 2012.
[21] B. Yinju, "Application of genetic BP network in earthquake and blasting identification," *Acta Seismologica Sinica*, vol. 2002, no. 5, pp. 516–524, 2002.
[22] Y. Horiuchi, J. Fujisaki, and N. Ishizuka, "Study on clinical factors involved in helicobacter pylori-uninfected, undifferentiated-type early gastric cancer," *Digestion*, vol. 96, no. 4, pp. 213–219, 2017.
[23] V. N. S. de Snyder, A. Acevedo, M. de Jesús Díaz-Pérez, and S. Garduño, "Understanding the sexuality of Mexican-born women and their risk for HIVIAIDS," *Psychol. Women Quart.*, vol. 24, no. 1, pp. 100–109, 2000.
[24] R. M. H. Dokht, H. Kao, R. Visser, and B. Smith, "Seismic event and phase detection using Time–Frequency representation and convolutional neural networks," *Seismological Res. Lett.*, vol. 90, no. 2A, pp. 481–490, Mar. 2019.
[25] L. Wanjun, J. Qingling, and Z. Chuang, "License plate location method based on CNN color image edge detection," *Acta automatica Sinica*, vol. 2009, no. 12, pp. 1503–1512, 2009.
[26] L. E. Hong, L. I. Huifang, W. A. N. G. Hua, and P. A. N. G. Xiongwen, "Food image recognition based on convolutional neural network," *J. South China Normal Univ. (Natural Sci. Ed.)*, vol. 51, no. 4, pp. 113–119, 2019.
[27] L. Jiazheng, W. Xuefeng, and W. Tian, "Research on the recognition of 5 bark texture images based on deep learning," *J. Beijing Forestry Univ.*, vol. 41, no. 4, pp. 146–154, 2019.
[28] Y. LeCun and Y. G. B. Hinton, "Deep learning," *Nature*, vol. 521, no. 4, pp. 436–444, 2015.
[29] T. Serre, L. Wolf, and T. Poggio, "Object recognition with features inspired by visual cortex," in *Proc. IEEE Comput. Soc. Conf. Comput. Vis. Pattern Recognit. (CVPR)*, San Diego, CA, USA, vol. 2, Jun. 2005, pp. 20–25.
[30] Q. Kong, D. T. Trugman, Z. E. Ross, M. J. Bianco, B. J. Meade, and P. Gerstoft, "Machine learning in seismology: Turning data into insights," *Seismological Res. Lett.*, vol. 90, no. 1, pp. 3–14, Jan. 2019.
[31] N. Wang and D.-Y. Yeung, "Learning a deep compact image representation for visual tracking," in *Proc. Adv. Neural Inf. Process. Syst.*, Lake Tahoe, NV, USA, Dec. 2013, pp. 809–817.
[32] W. Zhu and G. C. Beroza, "PhaseNet: A deep-neural-networkbased seismic arrival-time picking method," *Geophys. J. Int.*, vol. 216, no. 1, pp. 261–273, 2019.
[33] M. Joswig, "Pattern recognition for earthquake detection," *Bull. Seismol. Soc. Amer.*, vol. 80, no. 1, pp. 170–186, 1990.
[34] S. C. Turaga, J. F. Murray, V. Jain, F. Roth, M. Helmstaedter, K. Briggman, W. Denk, and H. S. Seung, "Convolutional networks can learn to generate affinity graphs for image segmentation," *Neural Comput.*, vol. 22, no. 2, pp. 511–538, Feb. 2010.

[35] Y. LeCun, K. Kavukcuoglu, and C. Farabet, "Convolutional networks and applications in vision," in *Proc. IEEE Int. Symp. Circuits Syst. (ISCAS)*, May 2010, pp. 253–256.
[36] Y. Zhou, H. Yue, Q. Kong, and S. Zhou, "Hybrid event detection and phase-picking algorithm using convolutional and recurrent neural networks," *Seismological Res. Lett.*, vol. 90, no. 3, pp. 1079–1087, May 2019.
[37] Y. G. Li, H. Wei, Z. Han, J. Huang, and W. Wang, "Deep learning-based safety helmet detection in engineering management based on convolutional neural networks," *Adv. Civil Eng.*, vol. 2020, Sep. 2020, Art. no. 9703560.
[38] L. Huang, J. Li, H. Hao, and X. Li, "Micro-seismic event detection and location in underground mines by using convolutional neural networks (CNN) and deep learning," *Tunnelling Underground Space Technol.*, vol. 81, pp. 265–276, Nov. 2018.
[39] G. S. Yogee, O. P. Mahela, K. D. Kansal, B. Khan, R. Mahla, H. H. Alhelou, and P. Siano, "An algorithm for recognition of fault conditions in the utility grid with renewable energy penetration," *Energies*, vol. 13, no. 9, p. 2383, May 2020.
[40] Z. E. Ross, M. Meier, and E. Hauksson, "P wave arrival picking and first-motion polarity determination with deep learning," *J. Geophys. Res. Solid Earth*, vol. 123, no. 6, pp. 5120–5129, Jun. 2018.
[41] Y. Yuan and D. Pu, "Machine learning methods for rockburst prediction state of the art review," *Int. J. Mining Sci. Technol.*, vol. 29, no. 4, pp. 44–49, 2019.

GUILI PENG was born in Tianjin, China, in 1981. He received the master's degree from the Southwest University of Science and Technology, Mianyang, Sichuan, China, in 2007. He is currently a Lecturer with Tianjin Chengjian University. His research interests include automatic control theory, and electrical and electronic technology. His main research interests include data signal processing and nuclear electronic technology.

XIANGUO TUO was born in Hunan, China, in 1965. He received the Ph.D. degree from the Chengdu University of Technology, Chengdu, China. He is currently a Professor with the Sichuan University of Science and Engineering. His research interests include nuclear technology theory, nuclear geophysical exploration methods, development of nuclear electronic instruments, radiation environment assessment, nuclide migration, and environmental monitoring and disaster warning methods.

TONG SHEN was born in Henan, China, in 1988. He received the Ph.D. degree from the Chengdu University of Technology, in 2019. He is currently a Lecturer with the Southwest University of Science and Technology. His research interests include geophysics and instrument science and technology. His main research interests include microseismic data signal processing, and research and design of seismic equipment.

JING LU (Graduate Student Member, IEEE) received the Dipl.-Ing. degree (master's degree) major in microelectronic and automation from the POLYTECH Montpellier, University of Montpellier, Montpellier, France, in 2014. He is currently pursuing the Ph.D. degree major in control science and engineering with the School of Information Engineering, Southwest University of Science and Technology. His research interests include automatic control theory and robotic. His main research interests include robot motion control and specialized robot design.